Load Balancing Game With Shadowing Effect for Indoor Hybrid LiFi/RF Networks

Yunlu Wang, *Student Member, IEEE*, Xiping Wu, *Member, IEEE*, and Harald Haas, *Member, IEEE*

***Abstract*— Light Fidelity (LiFi) is a recently proposed technology that uses 300 THz visible light spectrum for high speed wireless communications as well as providing illumination. Basically, a LiFi access point (AP) covers only a few square meters, enabling a dense deployment of LiFi APs to improve the network throughput. However, channel blockage and shadowing in conjunction with inter-cell interference compromise the connectivity and system throughput of LiFi networks. In this paper, a network structure that combines LiFi with the conventional radio frequency (RF) system is considered. Users experiencing strong blockages can be switched to the RF system to achieve a higher data rate. In this paper, blockages, random orientation of LiFi receivers, and the user data rate requirement are characterised to model a practical communication scenario. A novel load balancing (LB) scheme based on evolutionary game theory is proposed for hybrid LiFi/RF networks. The performance of the proposed scheme is comprehensively analyzed. Results show that compared to state-of-the-art LB algorithms, the proposed scheme greatly improves user satisfaction levels at reduced computational complexity. Also, an optimal orientation of LiFi receivers and blockage density in hybrid networks would maximize the users quality of service.**

***Index Terms*— Evolutionary game theory, hybrid network, LiFi, load balancing, RF, shadow**

I. Introduction

DUE to the exponentially increasing demand for mobile data traffic, the current indoor radio frequency (RF) systems tend to be overloaded. A potential solution is the hybrid network that integrates different wireless technologies to improve the network capacity. Light fidelity (LiFi), which uses existing light emitting diode (LED) lighting infrastructures for high speed wireless communications, has been considered to form a new tier within the future indoor hybrid networks [1]–[3]. One major advantage of such a hybrid network is that LiFi and RF signals do not interfere with each other since they use an entirely different part of the electromagnetic spectrum. LiFi can be regarded as nanometer wave (nmWave) wireless communication extending current millimeter wave (mmWave) wireless technologies. Compared with RF systems, LiFi can potentially provide a much higher level of signal-to-noise ratio (SNR) [4]. Also, LiFi can use a huge and unregulated bandwidth resource of up to 300 THz, 600,000 times larger than the 500 MHz WiGig (wireless gigabit alliance) channel in the industrial, scientific and medical (ISM) band. Using wavelength division multiplexing (WDM) in conjunction with off-the-shelf LEDs, LiFi is capable of providing data rates of 14 Gb/s [5]. In indoor environments, a single LiFi cell covers a few square meters due to propagation characteristics of light such as high path loss and low multipath reflections. Hence, multiple light sources are required to cover a large room, leading to a high spatial spectral efficiency in LiFi systems. In spite of the dense deployment of access points (APs), LiFi may not provide a uniform coverage in terms of data rate performance mainly due to inter-cell interference (ICI) and blockages [4]. Therefore, a hybrid LiFi/RF network is proposed to mitigate the spatial fluctuation of data rate offering a system throughput greater than that of stand alone LiFi or RF networks [2]. Most published research considers an ideal system model of hybrid networks, especially the LiFi channel model. In order to attain a more accurate evaluation of the system performance, three practical factors must be taken into account:

1) Blockage: In general, the signals of line of sight (LoS) paths contribute to most received signal power in a LiFi system. In an indoor scenario, opaque objects such as people and furniture can block the LoS optical channel and this would significantly compromise the data rate performance. Therefore, the shadowing effect in a LiFi system needs to be considered.

2) Receiving Orientation Angle (ROA): In most published research, the LiFi receiver is always assumed to be oriented perpendicularly upwards, and for simplicity the incidence angle is set equal to the angle of irradiation. However, it has been shown in [6] that this incidence angle varies depending on the users' behaviour pattern, and would significantly affect the receive SNR. Therefore a random ROA needs to be considered in the LiFi system model.

3) User Data Rate Requirement: Published research with respect to hybrid networks focuses on the improvement of system throughput and user fairness [1], [2], [7]. In general, each user has a required data rate in a short period to support certain wireless services such as browsing a web page, on-line video stream and voice over Internet protocol (VoIP). On the one hand, achieving a lower data rate than required would affect the quality of service (QoS) of users. On the other hand, a higher data rate than the requirement may lead to inefficient use of precious resources and possibly result in an overload of other cells. Therefore, user data rate requirements should be considered in the system load balancing (LB) for hybrid networks.

Manuscript received May 30, 2016; revised October 3, 2016 and January 15, 2017; accepted January 20, 2017. Date of publication March 13, 2017; date of current version April 7, 2017. This work was supported by EPSRC under Established Career Fellowship Grant EP/K008757/1. The associate editor coordinating the review of this paper and approving it for publication was M. S. Alouini.

The authors are with the Li-Fi Research and Development Centre of Edinburgh, Edinburgh University, EH9 3JL, U.K. (e-mail: yunlu.wang@ed.ac.uk; xiping.wu@ed.ac.uk; h.haas@ed.ac.uk).

Color versions of one or more of the figures in this paper are available online at http://ieeexplore.ieee.org.

Digital Object Identifier 10.1109/TWC.2017.2664821

1536-1276 © 2017 IEEE. Personal use is permitted, but republication/redistribution requires IEEE permission.
See http://www.ieee.org/publications_standards/publications/rights/index.html for more information.

Authorized licensed use limited to: CAMBRIDGE UNIV. Downloaded on November 18,2020 at 14:37:39 UTC from IEEE Xplore. Restrictions apply.

The system throughput and user satisfaction levels in hybrid LiFi/RF networks can be enhanced by using efficient LB techniques, which address two main issues: AP assignment (APA) and resource allocation (RA). In [1], [2], the APA and the RA are jointly optimised, and an iterative algorithm is given to find an optimal solution. In order to reduce the computational complexity, a LB scheme that separately optimises the APA and the RA is proposed in [7], [8], but the achievable data rates are significantly compromised. Therefore a novel LB scheme that can offer a proper performance/complexity trade-off is necessary. Moreover, when considering user data rate requirement, a piecewise function is normally needed to quantify the satisfaction of users because a data rate higher than the one required no longer increases the users' satisfaction level [9]. The conventional joint optimisation methods are NP-hard problems [1], [2]. Taking the user data rate requirement into account would further increase the complexity and result in a mathematically intractable problem. In this study, an evolutionary game theory (EGT) based LB scheme is proposed, where the problems of APA and RA are jointly handled. This algorithm accommodates the user data rate requirement for resource allocation, and a novel RA scheme that makes full use of the communication resources is proposed. This EGT algorithm can greatly improve the system throughput while achieving low computational complexity.

A. Evolutionary Game Theory

In the recent literature, game theory has been extensively applied to network selection and interference management problem in heterogeneous wireless networks [10]–[12]. The Nash equilibrium (NE) is the most commonly used solution to the non-cooperative game because it ensures that no player can improve its payoff without compromising another player. However, when there are multiple NEs in the game, a refined solution is required to ensure users' payoff reaching a stable status. Evolutionary equilibrium (EE), which is based on the EGT, can provide such a refined solution where a group of players will not change their chosen strategies over time [10].

In the EGT model, each user selects a strategy by replication and adapts its selection for a better payoff (i.e. user satisfaction) until no user can increase their payoff by unilaterally changing strategy. An EGT based method is used in [10] to solve the problem of network selection in an environment where multiple networks are available. In [11], the EGT based subcarrier and power allocation for small-cell networks are proposed. In [12], the authors used a stochastic geometry-based approach to analyse the stability of equilibrium of the evolutionary game in macro/micro heterogeneous wireless networks. In this study, an EGT based system load balancing scheme for an indoor LiFi/RF network is proposed with user data rate requirement taken into account. Different from conventional EGT based approaches, the proposed algorithm jointly deals with the APA and the RA rather than only focuses on the network selection. Specifically, the max-min fairness and the proportional fairness schedulers are used in the RA. Also, an enhanced proportional fairness scheduler is proposed to improve the efficiency of resource utilisation.

TABLE I
NOMENCLATURE

Parameters	Explanation
θ_{PD}	Maximal vertical ROA at LiFi receivers
$k_{\mu,\alpha}$	Time resource portion allocated to user μ by AP α
λ_μ	Data rate requirement of user μ
$\gamma_{\mu,\alpha}$	Data rate of the link between user μ and AP α
$\mathcal{S}_\mu$	Set of AP candidates in the EGT based LB scheme
N_{all}	Number of users in the hybrid network
N_α	Number of users served by AP α
N_{ap}	Number of APs in the hybrid network
β	Fairness coefficient in the utility function
$\pi_{\mu,\alpha}$	Payoff of user μ served by AP α
$\bar{\pi}_\alpha$	Average payoff of users served by AP α
$\bar{\pi}$	Global average payoff of all users
$p_\mu^{(t)}$	Mutation probability for a strategy shift in the t-th iteration
$\dot{\pi}_{\mu,\alpha}$	Estimated payoff if user μ switches host AP to α
I_{E}	Number of iterations for convergence in the EGT algorithm
N_{B}	Number of blockages in the simulation scenario
η	Blockage density (units/m^2)

B. Main Contributions

- An EGT based load balancing scheme is proposed for hybrid LiFi/RF networks where the following practical issues are considered: i). channel blockages; ii). LiFi ROA; iii). user data rate requirement. The proposed algorithm jointly handles the APA and the RA, and the optimality of this algorithm is analysed in this study.
- When considering user data rate requirement, conventional fairness schedulers such as max-min fairness and proportional fairness may lead to inefficient use of communication resources. In the proposed EGT based algorithm, an enhanced proportional fairness scheduler for resource allocation is proposed to avoid inefficient use of transmission resources. The performance of user satisfaction for both conventional and proposed fairness schedulers is evaluated by computer simulations.
- The effects of blockages and the ROA, which are unique channel characteristics of LiFi, are analysed in this study. To the best of the authors' knowledge, it is for the first time that an investigation on how these two issues affect the system load balancing in hybrid LiFi/RF networks is conducted.

The rest of the paper is organised as follows. The practical hybrid LiFi/RF network model is introduced in Section II. The EGT based load balancing scheme is given in Section III. The performance evaluation is presented in Section IV and conclusions are drawn in Section V. The nomenclature of the parameters that appear frequently in this paper is given in Table I.

II. HYBRID LIFI/RF NETWORK MODEL

A. System Setup

In this study, an indoor scenario covered by a hybrid LiFi/RF network is considered, where N_l LiFi APs and N_r RF APs are deployed. All of the LiFi and RF APs are connected to a central unit (CU) using optical fibres. In the LiFi system, each LiFi AP consists of several low power LEDs, and the total optical power of each LiFi AP is denoted by P_{opt}. The photon detector (PD) at each LiFi receiver may have horizontal and

Authorized licensed use limited to: CAMBRIDGE UNIV. Downloaded on November 18,2020 at 14:37:39 UTC from IEEE Xplore. Restrictions apply.

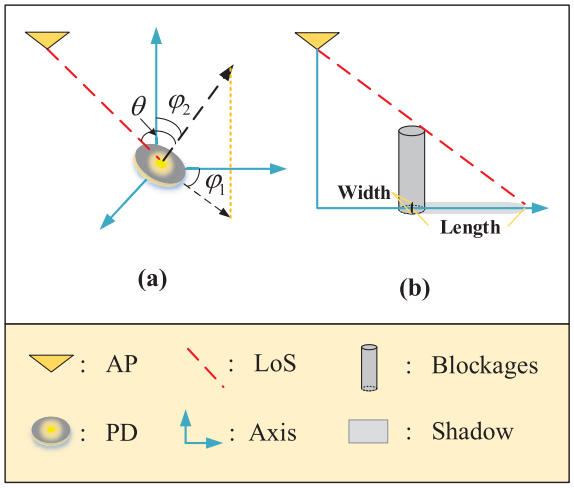

Fig. 1. Illustration of ROA and blockages.

vertical tilts, as shown in Fig. 1(a). In Cartesian coordinates, the direction vector of the PD can be expressed as:

$$\overrightarrow{\boldsymbol{d_1}} = (\cos(\varphi_1)\sin(\varphi_2), \sin(\varphi_1)\sin(\varphi_2), \cos(\varphi_2)), \quad (1)$$

where φ_1 is the horizontal ROA which follows a uniform distribution between 0° and 360°; and φ_2 is the vertical ROA which follows a uniform distribution between 0^o and θ_{PD}, where $0° \leq \theta_{\text{PD}} \leq 90°$ is the maximum vertical ROA. A PD of $\theta_{\text{PD}} = 0^o$ is perpendicular to the floor. The distance vector from a user to a LiFi AP is denoted by:

$$\overrightarrow{\boldsymbol{d_2}} = (x_a - x_u, y_a - y_u, z_a - z_u), \quad (2)$$

where (x_a, y_a, z_a) and (x_u, y_u, z_u) are the coordinates of the LiFi AP and the user, respectively. The angle of incidence to the PDs can be expressed as:

$$\theta = \arccos < \overrightarrow{\boldsymbol{d_1}}, \overrightarrow{\boldsymbol{d_2}} >, \quad (3)$$

where $<,>$ is the inner product operator. Due to the field of view (FoV) of the LED and PDs, each LiFi AP covers a confined cell, termed as an optical attocell. Since an attocell can significantly reduce the spread of signals outside a given zone determined by the light cone, LiFi APs are able to reuse the same bandwidth in a radical manner. Optical inter-cell interference (ICI) is treated as an additive noise [13]. In this study, a square lattice topology is used for the deployment of LiFi APs so as to model a regular lighting placement used in large offices and public places. Moreover, a RF system working at 2.4 GHz covers the whole indoor scenario. When more than one RF AP is considered, the RF ICI is not negligible. It is assumed that the RF APs use different channels, and the spectrum used by each RF AP is non-overlapping.

Assume that the channel state information (CSI) in both LiFi and RF systems changes slowly and is constant in a short period of T, which contains N_t transmission time intervals (TTIs). During a period of T, the load distribution is considered to be fixed in the hybrid network. In this study, user movement is not taken into account, and the EGT based dynamic load balancing scheme with handover will be subject to future research.

Time division multiple access (TDMA) is used at each LiFi and RF cell to serve multiple users [2]. The portion of the time resource allocated to user μ in a signal frame is denoted by $k_{\mu,\alpha}$, where α is the index of the serving AP and $k_{\mu,\alpha} \in [0, 1]$. The data rate requirement of each user during time T is denoted by λ_μ. The number of users is denoted by N_μ; the set of LiFi APs is denoted by $\mathcal{C}_\mathcal{L} = \{l |\ l \in [1, N_l], l \in \mathbb{N}\}$; the set of RF APs is denoted by $\mathcal{C}_\mathcal{R} = \{r |\ r \in [1, N_r], r \in \mathbb{N}\}$; and the total number of the APs is denoted as $N_{\text{ap}} = N_l + N_r$.

B. LiFi Channel Model With Blockages

In this study, the blockage caused by opaque objects in LiFi attocells is considered. According to [14], an object which generates a shadow in an indoor scenario is approximately modeled by a cylinder, 1.2 m (height) and 0.8 m (diameter). The shape of the shadow caused by this cylinder is assumed to be a rectangle. As shown in Fig. 1 (b), the length of the rectangle is defined as the distance between the cylinder bottom and the shadow of the cylinder top, and the width of the rectangle is the diameter of the cylinder. It is assumed that the PDs in the shadows cannot receive any LoS optical signal from the blocked LiFi APs.

The LiFi channel impulse response in the frequency domain can be modeled as [15]:

$$H_{\mu,\alpha}(f) = \begin{cases} (H_L + H_D(f))H_F(f), & \text{LoS not blocked} \\ H_D(f)H_F(f), & \text{LoS blocked,} \end{cases} \quad (4)$$

where H_L is the path loss of a LoS channel; $H_D(f)$ is the channel gain caused by multi-path propagation and diffuse effect; and $H_F(f)$ is the front-end device frequency response. The LoS channel fading follows [6]:

$$H_L = \begin{cases} \dfrac{(m+1)A_p\chi^2}{2\pi(z^2 + h_w^2)\sin^2\Theta_F} T_s(\theta)\cos^m(\phi)\cos(\theta), & \theta \leq \Theta_F \\ 0, & \theta > \Theta_F, \end{cases} \quad (5)$$

where m is the Lambertian index which is a function of the half-intensity radiation angle $\theta_{1/2}$, expressed as $m = -1/\log_2(\cos(\theta_{1/2}))$; A_p is the physical area of the receiver photo-diode; z is the horizontal distance from a LiFi AP to the optical receiver; h_w is the height of the room; ϕ is the angle of irradiation; θ is the angle of incidence to the PDs according to Eq. (3); Θ_F is the half angle of the receiver FoV; $T_s(\theta)$ is the gain of the optical filter; and χ is the refractive index. The diffuse component can be defined as [16]:

$$H_D(f) = \frac{\rho A_p e^{-j2\pi f \Delta T}}{A_r(1-\rho)(1 + j\frac{f}{f_c})}; \quad (6)$$

where A_r is the area of the indoor scenario surface; ρ is the reflectivity of the walls; ΔT is the delay between the LoS signal and the onset of the diffuse signals; and f_c is the cut-off frequency of the diffuse optical channel. The front-end device frequency response is modeled as follows [17]:

$$H_F(f) = \exp(-\frac{f}{1.44 f_0}), \quad (7)$$

Authorized licensed use limited to: CAMBRIDGE UNIV. Downloaded on November 18,2020 at 14:37:39 UTC from IEEE Xplore. Restrictions apply.

where f_0 is the 3 dB cut-off frequency of the front-end filtering effect.

In this study, the direct current (DC) biased optical orthogonal frequency division multiplexing (DCO-OFDM) is employed in the LiFi system [13]. The signal to interference and noise ratio (SINR) for user μ connected to a LiFi AP α can be written as:

$$\mathrm{SINR}_{\mu,\alpha}(f) = \frac{(\kappa P_{\mathrm{opt}} H_{\mu,\alpha}(f))^2}{\imath^2 N_{\mathrm{L}} B_{\mathrm{L}} + \sum_{i \in C_{\mathcal{L}} \cup C_{\mathcal{R}} \setminus \{\alpha\}} (\kappa P_{\mathrm{opt}} H_{\mu,i}(f))^2}, \tag{8}$$

where P_{opt} is the average transmitted optical power of LiFi AP; κ is the optical to electric conversion efficiency at the receivers; $\imath$ is the ratio of DC optical power to the square root of electric signal power, where $\imath = 3$ can guarantee approximately 0.3% of the signals are clipped so that the clipping noise can be neglected [13]; N_{L} is the noise power spectral density in LiFi links; B_{L} is the baseband modulation bandwidth used by each LiFi AP; $H_{\mu,\alpha}(f)$ is the channel gain in the frequency domain between user μ and the host LiFi AP α; and $H_{\mu,i}(f)$ is the channel gain in the frequency domain between user μ and the interfering LiFi AP i, according to Eq. (5).

C. RF Channel Model

An omni-directional transmit antenna is employed for the 2.4 GHz RF AP. Orthogonal frequency division multiplexing (OFDM) is used in the RF system, and the RF channel gain between user μ and RF AP α on each subcarrier is given by:

$$G_{\mu,\alpha}(f) = \sqrt{10^{\frac{-L(d)}{10}}} h_r, \tag{9}$$

where h_r is the small scale fading gain which has an independent identical Rayleigh distribution with average power 2.46 dB [18]; and $L(d)$ is the large-scale fading loss in decibels at the separation distance, d, which is given by [18]:

$$L(d) = \begin{cases} L_{\mathrm{FS}}(d) + X_{\mathrm{SF}}, & d < d_{\mathrm{BP}} \\ L_{\mathrm{FS}}(d_{\mathrm{BP}}) + 35 \log_{10}(d/d_{\mathrm{BP}}) + X_{\mathrm{SF}}, & d \geq d_{\mathrm{BP}}, \end{cases} \tag{10}$$

where $L_{\mathrm{FS}}(d) = 20\log_{10}(d) + 20\log_{10}(f) - 147.5$ (dB) is the free space loss up to a breakpoint distance $d_{\mathrm{BP}} = 10$ m, where f is the carrier frequency; and X_{SF} is the shadowing fading loss due to large scale blockage, which is 3 dB in typical indoor scenarios. Since there is no ICI in the RF system, the SINR is equivalent to SNR on each subcarrier, which can be expressed as:

$$\mathrm{SNR}_{\mu,r}(f) = \frac{|G_{\mu,\alpha}(f)|^2 P_{\mathrm{R}}}{\sigma^2}, \tag{11}$$

where P_{R} is the transmit power on each subcarrier; σ^2 is the variance of the additive white Gaussian noise (AWGN); and $G_{\mu,\alpha}(f)$ is the channel gain according to Eq. (9).

TABLE II
MODULATION AND CODING TABLE

min. SINR or SNR [dB]	Modulation	Code rate	Spectrum efficiency [bit/s/Hz]
-	-	-	0
1	QPSK	0.44	0.8770
3	QPSK	0.59	1.1758
5	16QAM	0.37	1.4766
8	16QAM	0.48	1.9141
9	16QAM	0.60	2.4063
11	64QAM	0.45	2.7305
12	64QAM	0.55	3.3223
14	64QAM	0.65	3.9023
16	64QAM	0.75	4.5234
18	64QAM	0.85	5.1152
20	64QAM	0.93	5.5547

D. Link Data Rate in Stand-Alone Networks

The number of OFDM sub-carriers used in LiFi and RF links is denoted by Q. Due to the channel fading in the frequency domain, adaptive M-QAM modulation is used on different OFDM sub-carriers [15]. In this study, the spectrum efficiency achieved on each subcarrier is obtained from the modulation and coding scheme (MCS) given in Table II [19]. Since the baseband bandwidth in the LiFi system is B_{L}, the OFDM bandwidth would be $2B_{\mathrm{L}}$, and the LiFi link data rate between user μ and AP α can be written as [20]:

$$Z_{\mu,\alpha} = \frac{2B_{\mathrm{L}}}{Q} \sum_{i=1}^{\frac{Q}{2}-1} q_{\mathrm{L}}(i), \tag{12}$$

where $q_{\mathrm{L}}(i)$ is the spectrum efficiency on sub-carrier i in the LiFi system, according to Eq. (8). The link communication data rate of RF can be written as:

$$\Upsilon_{\mu,\alpha} = \frac{B_{\mathrm{R}}}{Q} \sum_{j=0}^{Q-1} q_{\mathrm{R}}(j), \tag{13}$$

where $q_{\mathrm{R}}(j)$ is the spectrum efficiency on sub-carrier j in the RF system, according to Eq. (11).

In order to reduce the complexity of AP selection, the receivers only select from the candidate APs with highest link data rate performance in the stand-alone LiFi or RF system. Without loss of generality, it is assumed that the link data rates between user μ and the APs follows:

$$\begin{cases} Z_{\mu,l_1} \geq \ldots Z_{\mu,l_i} \geq Z_{\mu,l_{i+1}} \ldots \geq Z_{\mu,l_{N_l}}, & l_i \in C_{\mathcal{L}} \\ \Upsilon_{\mu,r_1} \geq \ldots \Upsilon_{\mu,r_j} \geq \Upsilon_{\mu,r_{j+1}} \ldots \geq \Upsilon_{\mu,r_{N_r}}, & r_j \in C_{\mathcal{R}}. \end{cases}$$

The AP resource of user μ can be defined as:

$$\mathcal{S}_\mu = \{l_1, r_1\}. \tag{14}$$

For simplicity, the link data rate between user μ and its candidate AP $\alpha \in \mathcal{S}_\mu$ is denoted by $\gamma_{\mu,\alpha}$, which can be expressed as:

$$\gamma_{\mu,\alpha} = \begin{cases} Z_{\mu,\alpha}, & \alpha \in C_{\mathcal{L}} \cap \mathcal{S}_\mu \\ \Upsilon_{\mu,\alpha}, & \alpha \in C_{\mathcal{R}} \cap \mathcal{S}_\mu. \end{cases}$$

Authorized licensed use limited to: CAMBRIDGE UNIV. Downloaded on November 18,2020 at 14:37:39 UTC from IEEE Xplore. Restrictions apply.

III. Load Balancing With Evolutionary Game

In this section, a new load balancing scheme is proposed, where the APA and the RA are formulated as an evolutionary game. Also, the replicator dynamic is used to model the strategy adaptation process for network load balancing [12]. The evolutionary equilibrium is considered to be the solution of the formulated load balancing game, and the stability and optimality of this algorithm are analysed.

A. Game Setup

The load balancing game can be formulated as follows:

1. Players Set ($\mathcal{U}$): The users in the hybrid network are the players in the game, and the number of players is denoted by $N_{\text{all}} = |\mathcal{U}|$.

2. Strategy Set ($\mathcal{S}_\mu$): The strategy set for each player is in accordance with Eq. (14). Each player can select one AP from $\mathcal{S}_\mu$.

3. Population: In the proposed game, each player should be allocated to an AP. The set of players connected to AP α ($\alpha \in \mathcal{C}_\mathcal{L} \cup \mathcal{C}_\mathcal{R}$) is denoted by $\mathcal{U}_\alpha$, where the number of players in this set is denoted by $N_\alpha = |\mathcal{U}_\alpha|$.

4. Payoff Function: The payoff of a player quantifies the satisfaction level of that player's action of AP selection, and this is considered as the user QoS. In general, player μ would be satisfied when its data rate is higher than the requirement λ_μ. Otherwise, the satisfaction level would decrease along with the data rate. Intuitively, the payoff function of user μ that is allocated to AP α can be written as:

$$\pi_{\mu,\alpha} = \min\left\{k_{\mu,\alpha}\frac{\gamma_{\mu,\alpha}}{\lambda_\mu},\ 1\right\}, \tag{15}$$

where $k_{\mu,\alpha}$ is the time resource portion provided by host AP α; and $\gamma_{\mu,\alpha}$ is the link data rate between player μ and AP α.

B. Resource Allocation

Since TDMA is used in this study, the time slot resource would be allocated to users in each cell by serving APs. Here the portion of time slot resource allocated by AP α for user μ is denoted by $k_{\mu,\alpha}$. In this study, a utility function in response to users' QoS and fairness is considered. This is referred to as β-proportional fairness function. This has been defined in [21] and is extensively used in [1], [3], [22]:

$$\psi_\beta(x) = \begin{cases} \ln(x), & \beta = 1 \\ \dfrac{x^{1-\beta}}{1-\beta}, & \beta \geq 0,\ \beta \neq 1, \end{cases} \tag{16}$$

where x is the user satisfaction level, defined as the user QoS; and β is the fairness coefficient. This utility function includes several well known fairness concepts [22]. For instance, when $\beta \to +\infty$, a max-min fairness scheduler is realised and when $\beta = 1$, a proportional fairness is achieved. Particularly, when $\beta = 0$, a linear utility function is obtained, which achieves a maximal system throughput. In this case, each AP only serves the user with the best channel state information (CSI) whereas the other users have zero data rates. This scheduler finally leads to an ineffective network load balancing. Thus, the situation of $\beta = 0$ is not under consideration.

In the cell covered by AP α, the resource allocation problem with the β-proportional fairness function can be formulated as:

$$\max_{k_{\mu,\alpha}} \sum_{\mu\in\mathcal{U}_\alpha} \psi_\beta\left(k_{\mu,\alpha}\frac{\gamma_{\mu,\alpha}}{\lambda_\mu}\right) \tag{17}$$

$$\text{s.t.} \sum_{\mu\in\mathcal{U}_\alpha} k_{\mu,\alpha} \leq 1; \tag{18}$$

where $\mathcal{U}_\alpha$ is the set of players allocated to AP α. The Lagrangian multiplier method is used to solve this problem. The Lagrangian function is given by:

$$F(k_{\mu,\alpha},\omega) = \sum_{\mu\in\mathcal{U}_\alpha} \psi_\beta\left(k_{\mu,\alpha}\frac{\gamma_{\mu,\alpha}}{\lambda_\mu}\right) + \omega\left(1 - \sum_{\mu\in\mathcal{U}_\alpha} k_{\mu,\alpha}\right), \tag{19}$$

where ω is the Lagrangian multiplier for the constraint in Eq. (18). The optimal $k_{\mu,\alpha}$ can be obtained by making the gradient of the Lagrangian function in Eq. (19) equal to 0, which is written as:

$$\frac{\partial F(k_{\mu,\alpha},\omega)}{\partial k_{\mu,\alpha}} = \frac{\partial \psi_\beta(k_{\mu,\alpha}\gamma_{\mu,\alpha}/\lambda_\mu)}{\partial k_{\mu,\alpha}} - \omega = 0, \tag{20}$$

where according to Eq. (16),

$$\frac{\partial \psi_\beta(k_{\mu,\alpha}\gamma_{\mu,\alpha}/\lambda_\mu)}{\partial k_{\mu,\alpha}} = \frac{\gamma_{\mu,\alpha}}{\lambda_\mu}\left(k_{\mu,\alpha}\frac{\gamma_{\mu,\alpha}}{\lambda_\mu}\right)^{-\beta}, (\beta > 0). \tag{21}$$

It can be derived from Eq. (20) and Eq. (21) that:

$$k_{\mu,\alpha} = \left(\frac{\gamma_{\mu,\alpha}}{\lambda_\mu}\right)^{\frac{1}{\beta}-1} \omega^{-\frac{1}{\beta}}. \tag{22}$$

According to Eq. (22) and Eq. (18), it can be further calculated that:

$$\omega^{\frac{1}{\beta}} = \sum_{\mu\in\mathcal{U}_\alpha}\left(\frac{\gamma_{\mu,\alpha}}{\lambda_\mu}\right)^{\frac{1}{\beta}-1}. \tag{23}$$

Combining Eq. (22) and Eq. (23), the optimum $k_{\mu,\alpha}$ can be expressed as:

$$k_{\mu,\alpha} = \frac{(\gamma_{\mu,\alpha}/\lambda_\mu)^{\frac{1}{\beta}-1}}{\sum_{i\in\mathcal{U}_\alpha}(\gamma_{i,\alpha}/\lambda_i)^{\frac{1}{\beta}-1}}\ (\beta > 0). \tag{24}$$

In this study, three fairness schedulers are considered, which are max-min fairness (MF), proportional fairness (PF) and enhanced proportional fairness (EPF).

1) MF: The MF is achieved with $\beta \to +\infty$ [22], and the optimal portion of allocated time resource can be expressed as:

$$k_{\mu,\alpha}^{(\text{MF})} = \lim_{\beta\to+\infty} \frac{(\gamma_{\mu,\alpha}/\lambda_\mu)^{\frac{1}{\beta}-1}}{\sum_{i\in\mathcal{U}_\alpha}(\gamma_{i,\alpha}/\lambda_i)^{\frac{1}{\beta}-1}} = \frac{(\gamma_{\mu,\alpha}/\lambda_\mu)^{-1}}{\sum_{i\in\mathcal{U}_\alpha}(\gamma_{i,\alpha}/\lambda_i)^{-1}}. \tag{25}$$

Combining Eq. (15) and Eq. (25), the user payoff with MF scheduler can be written as:

$$\pi_{\mu,\alpha}^{(\text{MF})} = \min\left\{\frac{1}{\sum_{i\in\mathcal{U}_\alpha}\lambda_i/\gamma_{i,\alpha}},\ 1\right\}, \tag{26}$$

where the operation $\min\{e_1, e_2\}$ represents the minimum between e_1 and e_2. It can be seen that all players served by AP α achieve equal payoffs.

Authorized licensed use limited to: CAMBRIDGE UNIV. Downloaded on November 18,2020 at 14:37:39 UTC from IEEE Xplore. Restrictions apply.

2) PF: The PF scheduler is realised by $\beta = 1$ [22]. According to Eq. (25), the optimal RA portion can be written as follows:

$$k_{\mu,\alpha}^{(\mathrm{PF})} = \left. \frac{(\gamma_{\mu,\alpha}/\lambda_\mu)^{\frac{1}{\beta}-1}}{\sum_{i\in\mathcal{U}_\alpha}(\gamma_{i,\alpha}/\lambda_i)^{\frac{1}{\beta}-1}} \right|_{\beta=1} = \frac{1}{N_\alpha}, \tag{27}$$

where N_α is the number of users in $\mathcal{U}_\alpha$. The user payoff of proportional scheduler is therefore expressed as:

$$\pi_{\mu,\alpha}^{(\mathrm{PF})} = \min\left\{ \frac{\gamma_{\mu,\alpha}}{\lambda_\mu N_\alpha},\ 1 \right\}. \tag{28}$$

In the PF scheduler, receivers in each cell share the same portion of time slot resource. Nevertheless, an inefficient use of resources may occur when users require low data rates. This issue will be handled by the EPF scheduler.

3) EPF: Unlike the PF scheduler, the EPF scheduler can avoid inefficient use of resources by allocating the redundant time slot resources of over-achieving users to those who achieve low user satisfaction. Specifically, the RA is initially undertaken through the PF scheduler, as shown in Eq. (27). After that, the redundant time slot resources of users achieving data rates higher than the requirements will be re-allocated to the other users via the PF scheduler to improve their user QoS performance. This re-allocation process is iteratively conduct until no user receives redundant resources. The EPF scheduler achieves a high level of resource utilisation as well as a near-proportional fairness. The RA process using the EPF scheduler is summarised in Algorithm 1. The payoff of each user achieved by the EPF scheduler can be expressed as:

$$\pi_{\mu,\alpha}^{(\mathrm{EPF})} = \frac{k_{\mu,\alpha}^{(\mathrm{EPF})}\gamma_{\mu,\alpha}}{\lambda_\mu}, \tag{29}$$

where $k_{\mu,\alpha}^{(\mathrm{EPF})}$ is the resource portion for user μ which can be obtained from Algorithm 1.

Algorithm 1 Enhanced Proportional Fairness Scheduler in Each Cell

1: Initialisation: The set of users served by AP α is denoted by $\mathcal{U}_{\mathrm{RA}} = \mathcal{U}_\alpha$; total time resource $K_r = 1$; and the set of users over-achieving is denoted by $\mathcal{U}_{\mathrm{Waste}} \neq \varnothing$.
2: **while** $\mathcal{U}_{\mathrm{RA}} \neq \varnothing$ and $\mathcal{U}_{\mathrm{Waste}} \neq \varnothing$ **do**
3: Allocate time resource to users in $\mathcal{U}_{\mathrm{RA}}$ using proportional fairness scheduler:

$$k_{\mu,\alpha}^{(\mathrm{EPF})} = \frac{K_r}{N_{\mathrm{RA}}}, \tag{30}$$

where N_{RA} is the number of users in $\mathcal{U}_{\mathrm{RA}}$.
4: Update $\mathcal{U}_{\mathrm{Waste}}$: $\mathcal{U}_{\mathrm{Waste}} = \{\mu |\ k_{\mu,\alpha}^{(\mathrm{EPF})}\gamma_{\mu,\alpha}/\lambda_\mu > 1, \mu \in \mathcal{U}_{\mathrm{RA}}\}$. The resource portion allocated to users in $\mathcal{U}_{\mathrm{Waste}}$ is changed to $k_{\mu,\alpha}^{(\mathrm{EPF})} = \lambda_\mu/\gamma_{\mu,\alpha}$.
5: Update $\mathcal{U}_{\mathrm{RA}}$: $\mathcal{U}_{\mathrm{RA}} = \mathcal{U}_{\mathrm{RA}} - \mathcal{U}_{\mathrm{Waste}}$.
6: Update total time resource:

$$K_r = K_r - \sum_{\mu\in\mathcal{U}_{\mathrm{Waste}}} \frac{\lambda_\mu}{\gamma_{\mu,\alpha}}. \tag{31}$$

7: **if** $\mathcal{U}_{\mathrm{RA}} = \varnothing$ **then**
8: The resource that have not been used can be allocated to all users with proportional fairness:

$$k_{\mu,\alpha}^{(\mathrm{EPF})} = k_{\mu,\alpha}^{(\mathrm{EPF})} + K_r/N_\alpha. \tag{32}$$

9: **end if**
10: **end while**

C. AP Assignment

In the context of the evolutionary game for load balancing, the players iteratively adapt their strategies of AP selection to enhance the payoffs. The duration of each iteration is considered as a TTI. The strategy adaptation process of AP selection and the corresponding population evolution can be modeled as follows. In the t-th iteration, the average payoff of players served by AP α is expressed as:

$$\bar{\pi}_\alpha^{(t,j)} = \frac{1}{N_\alpha}\sum_{\mu\in\mathcal{U}_\alpha}\pi_{\mu,\alpha}^{(t,j)},\ \ j \in \{\mathrm{MF}, \mathrm{PF}, \mathrm{EPF}\}, \tag{33}$$

where $\pi_{\mu,\alpha}^{(t,j)}$ is the payoff for user μ. The global average payoff of all players in this hybrid network can therefore be obtained:

$$\bar{\pi}^{(t,j)} = \frac{1}{N_{\mathrm{all}}}\sum_{\alpha\in\mathcal{C}_\mathcal{L}\cup\mathcal{C}_\mathcal{R}} N_\alpha\bar{\pi}_\alpha^{(t,j)},\quad j \in \{\mathrm{MF}, \mathrm{PF}, \mathrm{EPF}\}. \tag{34}$$

The AP selection strategy of each player is based on its previous payoff, the average payoff of each cell and the global average payoff in the last iteration, denoted by $\pi_{\mu,\alpha}^{(t-1,j)}$, $\bar{\pi}_\alpha^{(t-1,j)}$ and $\bar{\pi}^{(t-1,j)}$, respectively. The strategy shift for any player occurs randomly and follows the rule that the player with lower value of payoff would be more likely to change its strategy. This is termed as 'mutation and selection mechanism' in EGT [12]. Based on this principle, the mutation probability for a strategy shift in the t-th iteration is designed as:

$$p_\mu^{(t,j)} = \begin{cases} 1 - \dfrac{\pi_{\mu,\alpha}^{(t-1,j)}}{\bar{\pi}^{(t-1,j)}}, & \pi_{\mu,\alpha}^{(t-1,j)} < \bar{\pi}^{(t-1,j)} \\ 0, & \pi_{\mu,\alpha}^{(t-1,j)} \geq \bar{\pi}^{(t-1,j)}. \end{cases} \tag{35}$$

When a player is 'mutated', an AP selection for this player is required. The new AP is determined by maximising the estimated payoff in the current iteration, which can be expressed as:

$$\alpha^{(t,j)} = \arg\max_{i\in\mathcal{S}_\mu} \hat{\pi}_{\mu,\alpha}^{(t,j)} \tag{36}$$

$$\text{s.t. } \hat{\pi}_{\mu,\alpha}^{(t,j)} = \begin{cases} \pi_{\mu,i}^{(t-1,j)}, & i = \alpha^{(t-1,j)} \\ \dot{\pi}_{\mu,i}^{(t,j)}, & i \neq \alpha^{(t-1,j)} \end{cases}$$
$$j \in \{\mathrm{MF}, \mathrm{PF}, \mathrm{EPF}\}, \tag{37}$$

where $\alpha^{(t,j)}$ is the AP selected by player μ at the t-th iteration; $\dot{\pi}_{\mu,i}^{(t,j)}$ is the estimated payoff if the player is served by a different AP from $\alpha^{(t-1,j)}$ which here is denoted as υ for simplicity. The estimated payoff $\dot{\pi}_{\mu,\upsilon}^{(t,j)}$ is greatly related to the fairness achieving schedulers considered in this work as follows:

1) MF: According to Eq. (26), the payoff of users served by the same AP is equal to their average payoff. When player μ is served by AP υ, the total time resource for other players

Authorized licensed use limited to: CAMBRIDGE UNIV. Downloaded on November 18,2020 at 14:37:39 UTC from IEEE Xplore. Restrictions apply.

allocated to this AP would decrease to $1 - k_{\mu,\upsilon}$. Since each player served by υ ultimately achieves an equal payoff after player μ joins in. The estimated payoff of player μ can be written as:

$$\dot{\pi}_{\mu,\upsilon}^{(t,\mathrm{MF})} = (1 - k_{\mu,\upsilon})\bar{\pi}_{\upsilon}^{(t-1,\mathrm{MF})}. \tag{38}$$

Also, the payoff of user μ can be expressed as:

$$\dot{\pi}_{\mu,\upsilon}^{(t,\mathrm{MF})} = k_{\mu,\upsilon}\frac{\gamma_{\mu,\upsilon}}{\lambda_{\mu}}. \tag{39}$$

Combining Eq. (38) and Eq. (39), it can be derived that:

$$\dot{\pi}_{\mu,\upsilon}^{(t,\mathrm{MF})} = \frac{\gamma_{\mu,\upsilon}\bar{\pi}_{\upsilon}^{(t-1,\mathrm{MF})}}{\lambda_{\mu}\bar{\pi}_{\upsilon}^{(t-1,\mathrm{MF})} + \gamma_{\mu,\upsilon}}. \tag{40}$$

2) PF: In the PF scheduler, users in a specific cell achieve equal time resource portion. When a new user joins the cell served by AP υ in the current iteration, the allocated portion of resources for each user becomes:

$$k_{\mu,\upsilon}^{(t-1,\mathrm{PF})} = \frac{1}{N_{\upsilon}^{(t-1,\mathrm{PF})} + 1} = \frac{k_{\upsilon}^{(t-1,\mathrm{PF})}}{1 + k_{\upsilon}^{(t-1,\mathrm{PF})}}, \tag{41}$$

where $N_{\upsilon}^{(t-1,\mathrm{PF})}$ is the total number of users served by AP υ in the last iteration; and $k_{\upsilon}^{(t-1,\mathrm{PF})} = 1/N_{\upsilon}^{(t-1,\mathrm{PF})}$ is the corresponding resource portion of users according to Eq. (27). Therefore, the estimated payoff of player μ in the t-th iteration can be written as:

$$\dot{\pi}_{\mu,\upsilon}^{(t,\mathrm{PF})} = \min\left\{\frac{\gamma_{i,\upsilon}}{\lambda_i(N_{\upsilon}^{(t-1,\mathrm{PF})} + 1)},\ 1\right\}. \tag{42}$$

3) EPF: It has been shown that the EPF scheduler is able to enhance the average user payoff performance by minimising the excess of time slot resources while achieving a proportional fairness. The EPF scheduler results in varying RA per user depending on their requirements of time resources. When a player is 'mutated', a simple method to estimate user payoff is to use the expression in Eq. (42) with $k_{\upsilon}^{(t-1,\mathrm{EPF})} = 1/N_{\upsilon}^{(t-1,\mathrm{EPF})}$, which is applied in this study. The estimated payoff of player μ with EPF taken into account can be expressed as follows:

$$\dot{\pi}_{\mu,\upsilon}^{(t,\mathrm{EPF})} = \min\left\{\frac{\gamma_{i,\upsilon}}{\lambda_i(N_{\upsilon}^{(t-1,\mathrm{EPF})} + 1)},\ 1\right\}. \tag{43}$$

D. Load Balancing Algorithm

In the evolutionary game, players are randomly mutated with a probability according to Eq. (35). If a mutation occurs, the player selects an AP based on Eq. (36). On the one hand a player can possibly stay with the original AP when it experiences a mutation. On the other hand a new AP could be selected by players in each iteration. The parameters required to estimate the payoff for the three schedulers (MF, PF and EPF) are $\bar{\pi}_{\upsilon}^{(t-1,\mathrm{MF})}$ (MF) and N_{υ} (PF and EPF), respectively. If no strategy shift occurs for any player, the load balancing algorithm converges.

Lemma 1: In the proposed game, the load balancing algorithm always converges.

Proof: Without loss of generality, the average payoff of users served by each AP in the t-th iteration can be expressed as:

$$\bar{\pi}_{n_1}^{(t,j)} \le \ldots \bar{\pi}_{n_i}^{(t,j)} \le \bar{\pi}_{n_{i+1}}^{(t,j)} \ldots \le \bar{\pi}_{n_{N_{\mathrm{ap}}}}^{(t,j)},$$
$$n_i \in \mathcal{C}_{\mathcal{L}} \cup \mathcal{C}_{\mathcal{R}}, \quad j \in \{\mathrm{MF}, \mathrm{PF}, \mathrm{EPF}\}. \tag{44}$$

The maximal difference between two average payoffs is denoted as $w^{(t,j)} = \bar{\pi}_{n_{N_{\mathrm{ap}}}}^{(t,j)} - \bar{\pi}_{n_1}^{(t,j)}$. In the next iteration, the players served by AP $n_{N_{\mathrm{ap}}}$ would not change the AP because their mutation probability is zero according to Eq. (35), and no player would join the AP n_1 due to the low estimated payoff based on Eq. (36). Thus, it can be seen that $\bar{\pi}_{n_{N_{\mathrm{ap}}}}^{(t+1,j)} \le \bar{\pi}_{n_{N_{\mathrm{ap}}}}^{(t,j)}$ and $\bar{\pi}_{n_1}^{(t+1,j)} \ge \bar{\pi}_{n_1}^{(t,j)}$ would be satisfied, resulting in $w^{(t,j)} \ge w^{(t+1,j)}$. Also, based on Eq. (44), it can be seen that $w^{(t,j)} \ge 0$ is achieved. According to the monotonically bounded theorem, there is:

$$\lim_{t\to+\infty} w^{(t,j)} = w, \quad w \ge 0, \tag{45}$$

where w is a constant. After $w^{(t,j)}$ converges, the difference between $\bar{\pi}_{n_{N_{\mathrm{ap}}-1}}^{(t,j)}$ and $\bar{\pi}_2^{(t,j)}$ also follows the monotonically bounded theorem and will converge. By such analogy, the average payoffs for all APs tend to be constant. Thus the network load balancing can achieve convergence. ■

The proposed EGT load balancing algorithm contains the following steps: i) users change their strategies unilaterally to find better serving APs in the AP assignment step; 2) the users served by the same AP are allocated the time slot resource according to the RA schemes, i.e. MF, PF and EPF; 3) repeat step i) and ii) until no user can change the strategy unilaterally to improve their payoff. The EGT technique is often implemented in a distributed fashion to achieve low computational complexity. However, a distributed EGT algorithm requires coordination of all users. In particular, each user needs to keep sending their strategy selections back to the APs until the algorithm converges, and this process consumes communication resources. However, the EGT algorithm can also be realised in a centralised manner, where the central unit (CU) undertakes the AP selection for users virtually following the EGT algorithm. After the CU works out the final AP selection results, users will be assigned to their serving APs for data transmission. An advantage is that the EGT algorithm for system load balancing can be carried out rapidly by consuming few communication resources in a centralised network. In this study, an indoor hybrid LiFi/RF network is considered. An EGT based centralised load balancing algorithm is proposed, where the CU selects the AP for each user in each iteration based on the users' CSI. This approach supports typical software defined networking (SDN) architectures [23]–[25]. The EGT-based centralised load balancing algorithm is summarised in Algorithm 2.

E. Evolutionary Equilibrium and Optimality Analysis

Definition 1: A strategy profile $\mathcal{A}_{\mu} = \{\alpha_{\mu} | \mu \in \mathcal{U}\}$ is an Evolutionary Equilibrium (EE) (referred to as the Nash Equilibrium in the evolutionary game [12]) of the proposed load balancing game if at the equilibrium $\mathcal{A}_{\mu}$, no player

Authorized licensed use limited to: CAMBRIDGE UNIV. Downloaded on November 18,2020 at 14:37:39 UTC from IEEE Xplore. Restrictions apply.

Algorithm 2 EGT Based Centralised Load Balancing Algorithm Using MF, PF and EPF Schedulers

1: Initialisation: A random AP from $\mathcal{S}_\mu$ is assigned to player μ; each AP allocates the time resource to the connected players using one of the three fairness schemes; the CU calculates the average payoff of each player $\pi_{\mu,\alpha}^{(0,j)} = \bar{\pi}_\alpha^{(0,j)}$, the global average payoff $\bar{\pi}^{(0,j)}$ with $j \in \{\text{MF}, \text{PF}, \text{EPF}\}$, k_υ and $k_\upsilon^{\max}$; and $t \leftarrow 1$. This algorithm is executed by the CU.
2: **for all** each player $\mu \in \mathcal{U}$ **do**
3: The CU calculates the mutation probability $p_{\mu 1}^{(t,j)}$ according to Eq. (35);
4: The CU generates a random number with uniform distribution between 0 and 1, denoted as δ.
5: **if** $\delta < p_\mu^{(t,j)}$ **then**
6: The mutation occurs and player μ is assigned to an AP based on Eq. (36).
7: **else**
8: Player μ is still assigned to the original AP.
9: **end if**
10: **end for**
11: **for all** each AP $\alpha \in \mathcal{C}_\mathcal{L} \cup \mathcal{C}_\mathcal{R}$ **do**
12: The CU calculates the time resource portion for players in each cell, according to Eq. (25), (27) and Algorithm. 1.
13: **end for**
14: The CU stores the parameters $\bar{\pi}_\upsilon^{(t,\text{MF})}$ and $N_\upsilon^{(t,\text{PF})}$ and $N_\upsilon^{(t,\text{EPF})}$ $(\upsilon \in \mathcal{C}_\mathcal{L} \cup \mathcal{C}_\mathcal{R})$ for payoff estimation.
15: $t \leftarrow t + 1$ and repeat from Step 2 until no AP switch occurs.

can further increase their payoff by unilaterally changing its strategy, i.e.:

$$\pi_{\mu,\alpha_\mu} \geq \pi_{\mu,\beta_\mu}, \quad \alpha_\mu \neq \beta_\mu, \ \alpha_\mu, \beta_\mu \in \mathcal{S}_\mu \tag{46}$$

where $\pi_{\mu,x}$ represents the payoff function for user μ allocated to AP x, according to Eq. (15).

It can be seen that when network load balancing converges, an EE is achieved. According to Lemma 1, the EE has the perfect self-stability property, and thus the players at the EE can achieve a mutually satisfactory solution. As a consequence, the EE can be regarded as the solution of the proposed evolutionary game. However, this does not mean that the optimal solution of maximising the average payoff of users has been achieved. Since a closed-form optimal solution of system load balancing is mathematically intractable, an exhaustive search is used to find this global optimum.

When considering N_{all} users and N_{ap} APs in the hybrid LiFi/RF network, there are $N_{\text{ap}}^{N_{\text{all}}}$ possibilities of AP assignments, which are denoted by $\mathbf{g}^{(i)}$, $i = 1, 2 \ldots N_{\text{ap}}^{N_{\text{all}}}$. Given a certain $\mathbf{g}^{(i)}$, the time resource portions using MF, PF and EPF schedulers can be computed based on Eq. (25), (27) and Algorithm 1, respectively. Subsequently, the global optimum of the system load balancing problem can be determined using an exhaustive search. The ratios of the payoffs achieved by the EGT algorithm to the global optima

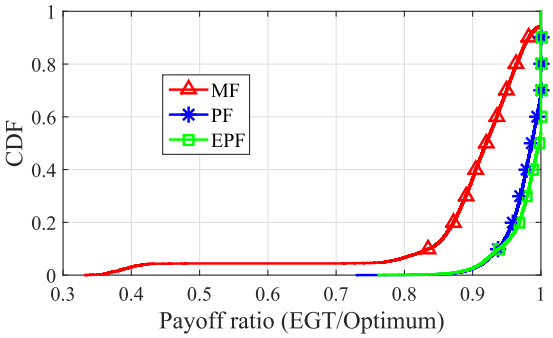

Fig. 2. Ratios of EGT payoffs to the global optima (1000 times of independent and identical simulations are considered).

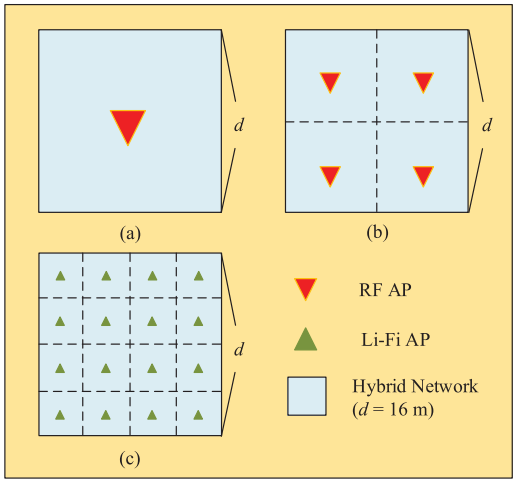

Fig. 3. Square topology for LiFi and RF network: (a). 1 RF AP; (b). 4 RF APs; (c). 16 LiFi APs.

are shown in Fig. 2. It can be seen that the EGT algorithm with three fairness achieving schedulers has a performance close to the optimum. Specifically, 70% of players using the MF scheduler can achieve a payoff over 90% of the global optimum. The PF and EPF schedulers have better performance than MF, where the payoff achieved by 80% of players is less than 5% close to the optimum. Therefore, it can be concluded that the EGT technique achieves near-optimal performance.

IV. Performance Evaluation

A. System Setup

In this study, a 16 m $\times$ 16 m indoor office space is considered. Two RF AP deployment scenarios are used as shown in Fig. 3 (a-b), and the LiFi AP deployment is shown in Fig. 3 (c). The users and the blocking objects are uniformly distributed, and the number of objects is denoted by N_{B}. The required data rate of each user follows a Poisson distribution with the parameter λ. The vertical ROA of each PD follows a uniform distribution ranging between 0 and θ_{PD}. In this study, the period of interest T is set to be 500 ms [26], and the channels and the data rate requirements of users are assumed to be fixed in this duration. According to [27], the TTI is set to be 2 ms. As a consequence, the maximum iteration number

Authorized licensed use limited to: CAMBRIDGE UNIV. Downloaded on November 18,2020 at 14:37:39 UTC from IEEE Xplore. Restrictions apply.

TABLE III
SIMULATION PARAMETERS

Name of Parameters	Value
Height of the room, h_w	2 m
Optical transmit power in the LiFi system, P_{opt}	10 W
Modulation bandwidth for LED lamp, B_{L}	100 MHz
Noise power spectral density of LiFi, N_{L}	10^{-21} A^2/Hz
The physical area of a PD, A_p	1 cm^2
Half-intensity radiation angle, $\theta_{1/2}$	60 deg.
Gain of optical filter, $T_s(\theta)$	1.0
Refractive index, χ	1.5
Cut-off frequency of diffuse optical channel, f_c	30 MHz
Cut-off frequency of front-end filtering effect, f_0	30 MHz
Optical to electric conversion efficiency, κ	0.53 A/W
Transmit power for each RF AP, P_{R}	20 dBm
Total transmitted bandwidth in RF system, B_{R}	80 MHz
Noise power of RF, σ^2	-57 dBm

of the proposed algorithm is 250. Other parameters related to the simulation are given in Table III. The payoff in the proposed algorithm is considered as the user QoS, which is between 0 and 1. When payoff is 0, users achieve zero data rates. When payoff is 1, users achieve data rates higher than or equal to the requirements.

In order to evaluate the performance of the proposed EGT based LB scheme, three benchmark algorithms are implemented for comparison:

1) Joint Optimisation Algorithm (JOA): In the JOA benchmark, APA and RA are jointly optimised with proportional fairness considered [1], [2], [19], [22], which is formulated as follows:

$$\max_{g_{\mu,\alpha},k_{\mu,\alpha}} \sum_{\mu\in\mathcal{U}}\sum_{\alpha\in\mathcal{C}_{\mathcal{L}}\cup\mathcal{C}_{\mathcal{R}}} g_{\mu,\alpha}\log(k_{\mu,\alpha}\gamma_{\mu,\alpha}/\lambda_\mu) \tag{47}$$

$$s.t.\ \sum_{\mu\in\mathcal{U}} g_{\mu,\alpha}k_{\mu,\alpha} \le 1 \quad \forall\alpha\in\mathcal{C}_{\mathcal{L}}\cup\mathcal{C}_{\mathcal{R}};$$

$$\sum_{\alpha\in\mathcal{C}_{\mathcal{L}}\cup\mathcal{C}_{\mathcal{R}}} g_{\mu,\alpha} = 1 \quad \forall\mu\in\mathcal{U};$$

$$g_{\mu,\alpha}\in\{0,1\},\quad k_{\mu,\alpha}\in[0,1],\ \forall\mu\in\mathcal{U},\ \forall\alpha\in\mathcal{C}_{\mathcal{L}}\cup\mathcal{C}_{\mathcal{R}}, \tag{48}$$

where $g_{\mu,\alpha}$ is a binary number which equals 1 when user μ is connected to AP α, and otherwise it is 0; $k_{\mu,\alpha}$ is the time resource portion provided by host AP α; $\gamma_{\mu,\alpha}$ is the link data rate between player μ and AP α; and λ_μ is the required data rate of user μ. This optimisation problem can be solved by a dual decomposition approach, and the solution is given in [2].

2) Threshold-Based Access Algorithm (TAA): In the TAA benchmark, the APA and the RA are separately optimised. Specifically, the APA is determined by using an optimal data rate threshold and the RA is performed using the proportional fairness scheduler [7].

3) Random Access Algorithm (RAA): In the RAA benchmark, APA and RA are also undertaken separately. Different from the TAA, each user randomly chooses the AP from $\mathcal{S}_\mu$ in the APA step. In the RA step, the RAA is conducted in the same way as the TAA.

TABLE IV
COMPUTATION COMPLEXITY

Algorithm	Addition	Multiplication	Exponentiation
EGT(MF,PF&EPF)	$O(N_{\text{all}}N_{\text{ap}}I_{\text{E}})$	$O(N_{\text{all}}N_{\text{ap}}I_{\text{E}})$	0
JOA	$O(N_{\text{all}}N_{\text{ap}}I_{\text{J}})$	$O(N_{\text{all}}N_{\text{ap}}I_{\text{J}})$	$O(N_{\text{all}}N_{\text{ap}}I_{\text{J}})$
TAA	$O(N_{\text{all}}N_{\text{ap}})$	$O(N_{\text{all}})$	0
RAA	$O(N_{\text{all}})$	$O(N_{\text{all}})$	0

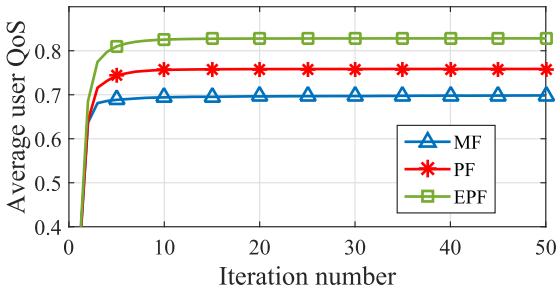

Fig. 4. Average user QoS corresponding to the iteration number (1 RF AP, $\lambda = 25$ Mb/s, $N_{\text{B}} = 10$, $\theta_{\text{PD}} = 0$, $N_{\text{all}} = 200$ and FoV $= 90°$).

B. Complexity Analysis

As shown in Fig. 4, the proposed EGT algorithm reaches a steady state after several iterations. Specifically, the number of iterations for convergence is denoted by I_{E}, and I_{E} is around 10 for all of the curves shown in Fig. 4. During the interval T, there are 250 TTIs, and only 10 TTIs are taken for convergence. Therefore 96% of the TTI can be used for signal transmission.

In this study, JOA, TAA and RAA are simulated as the benchmarks for performance evaluation. The computational complexity of these algorithms is summarised in Table IV, where I_J is the iteration number in JOA [3]. The EGT algorithm with three RA schedulers achieves a lower complexity than JOA because the EGT algorithm includes no exponential operation but JOA does. However, the complexity of the EGT algorithm is higher than TAA and RAA due to the iterative computation.

C. Evaluation of User QoS

The user QoS performance with different RF AP deployments is shown in Fig. 5. It can be found that the user QoS with 1 RF AP exhibits similar performance to the case with 4 RF APs. On the one hand, 4 RF APs can reduce the path loss between users and APs, resulting in a higher receive SINR than in the case of 1 RF AP. On the other hand, according to Eq. (14), each user only uses the best LiFi and RF AP as the candidates for AP assignment, and the best LiFi attocell is generally covered by the best RF AP. In the network with 1 RF AP, when a LiFi attocell is overloaded, users in this attocell will be transferred to the RF cell so that the system load can be well balanced. However, in the network with 4 RF APs, since each user can only be served by either the best RF AP or the best LiFi AP, the hybrid network would be naturally divided into four independent regions. The users in one region cannot be served by the APs in other regions. Therefore, it is difficult to achieve an efficient load balancing over the entire network, resulting in a decrease in the user QoS to the scenario with 1 RF AP. Accordingly, even though the

Authorized licensed use limited to: CAMBRIDGE UNIV. Downloaded on November 18,2020 at 14:37:39 UTC from IEEE Xplore. Restrictions apply.

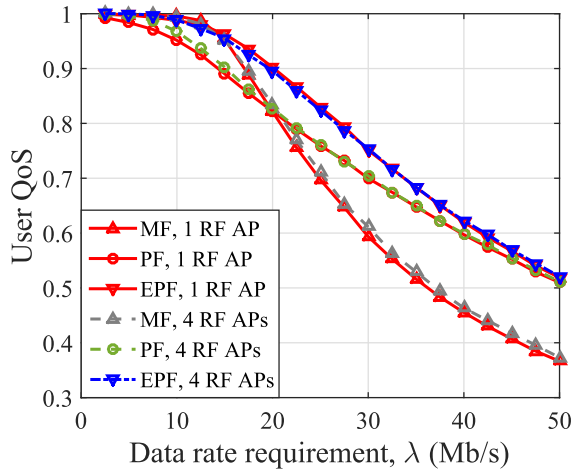

Fig. 5. Evaluation of user QoS with different RF setups. ($N_{\mathrm{B}} = 10$, $\theta_{\mathrm{PD}} = 0$, $N_{\mathrm{all}} = 200$ and FoV $= 90°$).

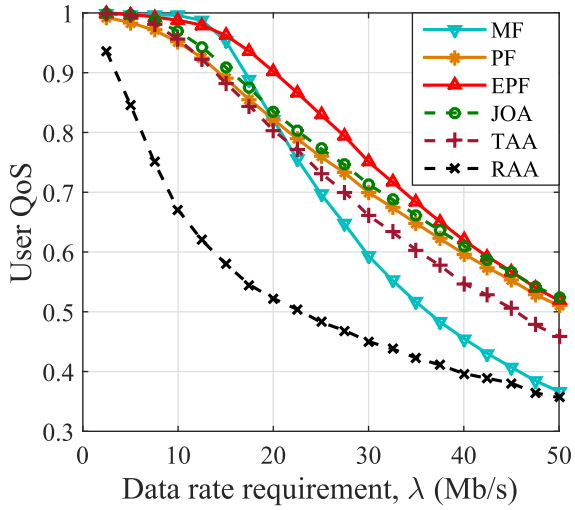

Fig. 6. Evaluation of user QoS achieved by different load balancing algorithms. (1 RF AP, $N_{\mathrm{B}} = 10$, $\theta_{\mathrm{PD}} = 0$, $N_{\mathrm{all}} = 200$ and FoV $= 90°$).

scenario with 4 RF APs provides users with a low path loss and a high level of SINR, the user QoS cannot be significantly enhanced over the scenario with 1 RF AP.

The average QoS as a function of required user data rate is shown in Fig. 6. It can be seen that the EGT algorithm with EPF outperforms the other schemes. In addition, the MF algorithm results in a steeper slope of user QoS than the PF algorithm, which attains a better user QoS with $\lambda \leq 25$ Mb/s. Compared with the three benchmark systems where the proportional fairness is taken into account, the proposed EGT algorithm with PF performs between JOA and TAA/RAA. However, when the EPF scheme is used in the EGT based algorithm, the user QoS is much higher than achieved by all benchmark techniques. The reason for this is that it minimises the inefficient use of transmission resources. In this study, it is assumed that the user QoS should be at least greater than 0.9 in order to guarantee the basic requirement of wireless services. It can be seen that in the hybrid LiFi/RF network with 200 users, an average user data rate of 20 Mb/s can be achieved by the EGT based algorithm.

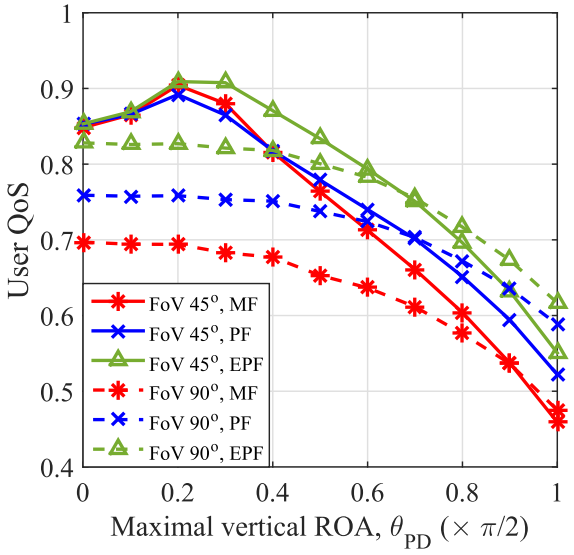

Fig. 7. User QoS with maximal vertical ROA θ_{PD}. (1 RF AP, $N_{\mathrm{B}} = 10$, $N_{\mathrm{all}} = 200$, $\lambda = 25$ Mb/s).

D. Effect of Vertical ROA

The receive SINR of LiFi is affected by the vertical ROA, φ_2. As shown in Section II.A, φ_2 follows a uniform distribution ranging between 0 and θ_{PD}, where θ_{PD} is the maximal vertical ROA (MVR). In the LiFi system, the vertical ROA is able to affect the angle of incidence of LiFi signals. When the angle of incidence is less than the FoV, LiFi signals can be received by the receivers. Otherwise, users can only be served by the RF APs. The effect of the MVR, θ_{PD}, on the performance of user payoff (or user QoS) is shown in Fig. 7. When the FoV is 45°, the QoS firstly increases than decrease with an increase in θ_{PD}. The optimum is attained approximately at $\theta_{\mathrm{PD}} = 25°$. On the one hand, when the vertical ROA tends to be zero, users at the edge of LiFi attocells may achieve a larger angle of incidence than FoV so that they can only be served by the RF AP, resulting in an inefficient load balancing. On the other hand, a large θ_{PD} will lead to a severe path loss of LiFi signals, which decreases the LiFi data rates. With FoV $= 90°$, the angle of incidence of users at any location can basically be less than the FoV. Therefore, the user QoS decreases with an increase in θ_{PD} due to the path loss effects in the LiFi system.

Here a comparison of user QoS between $\theta_{\mathrm{PD}} = 0$ and 30° is made and demonstrated in Fig. 8, where the FoV is 45°. In the case of $\theta_{\mathrm{PD}} = 0$, LiFi receivers are perpendicular to the ground, and the angle of irradiance is equal to the angle of incidence in the LoS optical channel. Since users have a FoV of 45°, they can only receive LoS LiFi signals in a confined area, where the angle of irradiance of signals from LiFi APs should be less than 45°. This confined area is defined as the serving area. It can be seen that with $\theta_{\mathrm{PD}} = 0$, the user QoS mainly falls into two different ranges that are $0.1 \leq \mathrm{QoS} \leq 0.6$ and $\mathrm{QoS} = 1$, corresponding to the two situations that are users in the serving area and users outside the area. However, when users have a vertical ROA ranging from 0 to 30° ($\theta_{\mathrm{PD}} = 30°$), each LiFi AP is capable of serving users with a maximal angle of irradiance as large as 75°, leading to an

Authorized licensed use limited to: CAMBRIDGE UNIV. Downloaded on November 18,2020 at 14:37:39 UTC from IEEE Xplore. Restrictions apply.

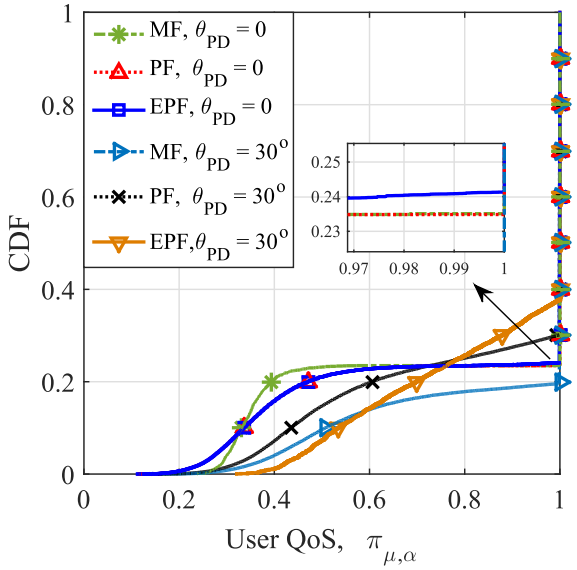

Fig. 8. CDF of user QoS achieved by EGT algorithms. (1 RF AP, $N_B = 10$, $N_{all} = 200$, FoV $= 45°$ and $\lambda = 25$ Mb/s).

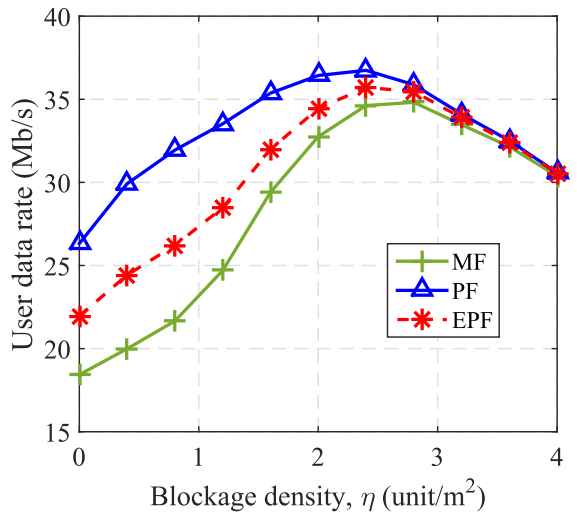

Fig. 9. Average data rate with different blockage densities. (1 RF AP, $N_{all} = 200$, FoV $= 90°$, $\theta_{PD} = 0$ and $\lambda = 25$ Mb/s).

enhancement of system load balancing. Therefore, it can be concluded that a proper vertical ROA in conjunction with a small FoV can improve the user QoS.

E. Effect of Blockage and Shadow

In this subsection, the shadowing effect resulting from blockages in the LiFi system is studied. The number of blockages are denoted by N_B, and the blockage density is defined as $\eta = N_B/S$, where S is the area of the simulation scenario. The average user data rate corresponding to the blockage density is shown in Fig. 9. The data rate of user μ is denoted by $D_\mu = k_{\mu,\alpha}\gamma_{\mu,\alpha}$, where α is the serving AP of user μ. It can be seen that the average user data rate is a concave function with respect to the blockage density, η. With a small value of η, users served by LiFi may experience interference from neighbouring LiFi APs. When η increases, the interference signals are more likely to be blocked and the achievable SINR in LiFi channels is therefore improved.

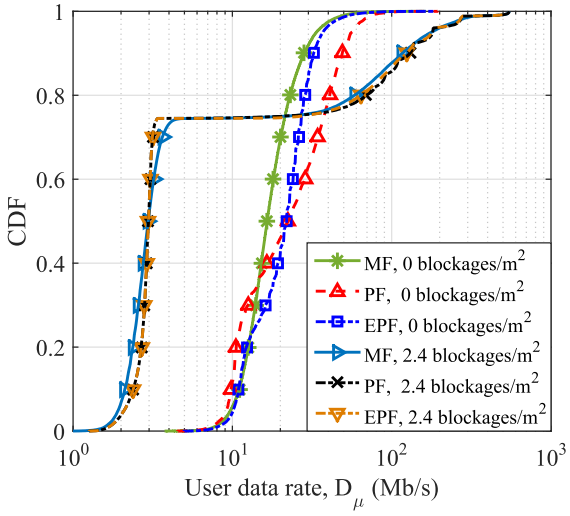

Fig. 10. CDF of user data rate with different blockage densities. (1 RF AP, $N_{all} = 200$, FoV $= 90°$, $\theta_{PD} = 0$ and $\lambda = 25$ Mb/s).

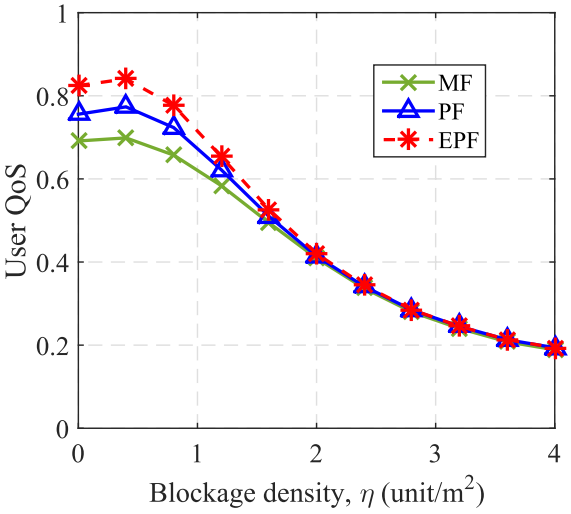

Fig. 11. Average user QoS with different blockage densities. (1 RF AP, $N_{all} = 200$, FoV $= 90°$, $\theta_{PD} = 0$ and $\lambda = 25$ Mb/s).

If the expected LiFi signals are blocked, the RF APs will be automatically allocated to those users by the CU. As shown in Fig. 9, the optimal data rate appears at $\eta = 2.4$. However, a further increase of η results in a decrease in the average data rate. This is because most of the users have to be allocated to the RF APs due to the blockage of LiFi LoS channels, which leads to a reduction of network throughput.

For different blockage situations, the CDF of the user data rate is shown in Fig. 10. It can be seen that the achievable data rates with blockages have a much larger range than those without blockages. When η is set to be 2.4 unit/m^2 (the optimal η in Fig. 9), the user data rates would basically be classified into two groups: [0, 4] Mb/s and [30, 600] Mb/s. Compared with the non-blockage case, 72% of the users in the blockage scenario experience a data rate degradation, while the remaining users achieve a significant data rate improvement. This means that although a blockage density of 2.4 unit/m^2 results in the largest average user data rate, more than half of the users in this case have to be served by RF APs

Authorized licensed use limited to: CAMBRIDGE UNIV. Downloaded on November 18,2020 at 14:37:39 UTC from IEEE Xplore. Restrictions apply.

and achieve a low data rate. Moreover, 28% of the users can obtain plenty of LiFi communication resources but their achievable data rates are much higher than required. Fig. 11 shows that when considering the required data rate of users, the QoS increases at the low blockage densities but decreases with a further increase in η. This indicates that an increase in blockage density cannot provide a better user experience despite achieving an improvement of the sum data rate.

V. Conclusion

In this study, in order to model a practical hybrid LiFi/RF network scenario, three factors are taken into account: blockages, LiFi ROA and user data rate requirement. An EGT based load balancing algorithm is proposed to improve the user QoS. Also, an enhanced proportional fairness scheduler is proposed to maximise the usage of communication resources in the RA step. The effects of the maximal vertical ROA and blockages on the hybrid network are evaluated and discussed. Three conclusions are drawn based on the simulation results: (i) The proposed EGT load balancing algorithm achieves a better performance/complexity trade-off than the conventional algorithms. In addition, when the EPF scheme is used, a high level of user QoS can be attained due to a more efficient exploitation of transmission resources; (ii) When the FoV of LiFi receivers is 90°, the average user QoS decreases with an increase in the maximal vertical ROA θ_{PD}. However, when considering a small FoV, there is an optimum of the maximal vertical ROA that can optimise the QoS performance, leading to a better system load balancing than attainable in the non-ROA case; (iii) An optimal blockage density of $\eta = 2.4$ unit/m^2 can maximise the system sum data rate. However, when considering user data rate requirement, the user QoS decreases with an increase in η as the blockages cause an inefficient allocation of communication resources.

References

[1] X. Li, R. Zhang, and L. Hanzo, "Cooperative load balancing in hybrid visible light communications and WiFi," *IEEE Trans. Commun.*, vol. 63, no. 4, pp. 1319–1329, Apr. 2015.

[2] Y. Wang and H. Haas, "Dynamic load balancing with handover in hybrid Li-Fi and Wi-Fi networks," *J. Lightw. Technol.*, vol. 33, no. 22, pp. 4671–4682, Nov. 15, 2015.

[3] F. Jin, R. Zhang, and L. Hanzo, "Resource allocation under delay-guarantee constraints for heterogeneous visible-light and RF femtocell," *IEEE Trans. Wireless Commun.*, vol. 14, no. 2, pp. 1020–1034, Feb. 2014.

[4] C. Chen, D. Basnayaka, and H. Haas, "Downlink performance of optical attocell networks," *J. Lightw. Technol.*, vol. 34, no. 1, pp. 137–156, Jan. 1, 2016.

[5] D. Tsonev, S. Videv, and H. Haas, "Towards a 100 Gb/s visible light wireless access network," *Opt. Exp.*, vol. 23, no. 2, pp. 1627–1637, Jan. 2015.

[6] J. M. Kahn and J. R. Barry, "Wireless infrared communications," *Proc. IEEE*, vol. 85, no. 2, pp. 265–298, Feb. 1997.

[7] Y. Wang, D. A. Basnayaka, and H. Haas, "Dynamic load balancing for hybrid Li-Fi and RF indoor networks," in *Proc. IEEE Int. Conf. Commun. Workshop (ICCW)*, London, U.K., Jun. 2015, pp. 1422–1427.

[8] D. A. Basnayaka and H. Haas, "Hybrid RF and VLC systems: Improving user data rate performance of VLC systems," in *Proc. IEEE 81st Veh. Technol. Conf. (VTC)*, Glasgow, U.K., May 2015, pp. 1–5.

[9] Y. Wang, X. Wu, and H. Haas, "Distributed load balancing for Internet of Things by using Li-Fi and RF hybrid network," in *Proc. IEEE 26th Annu. Int. Symp. Pers., Indoor, Mobile Radio Commun. (PIMRC)*, Hong Kong, Aug. 2015, pp. 1289–1294.

[10] D. Niyato and E. Hossain, "Dynamics of network selection in heterogeneous wireless networks: An evolutionary game approach," *IEEE Trans. Veh. Technol.*, vol. 58, no. 4, pp. 2008–2017, May 2009.

[11] M. Bennis, S. Guruacharya, and D. Niyato, "Distributed learning strategies for interference mitigation in femtocell networks," in *Proc. IEEE Global Telecommun. Conf. (GLOBECOM)*, Houston, MA, USA, Dec. 2011, pp. 1–5.

[12] P. Semasinghe, E. Hossain, and K. Zhu, "An evolutionary game for distributed resource allocation in self-organizing small cells," *IEEE Trans. Mobile Comput.*, vol. 14, no. 2, pp. 274–287, Feb. 2015.

[13] S. Dimitrov and H. Haas, *Principles of LED Ligh t Communications: Towards Networked Li-Fi*. Cambridge, U.K.: Cambridge Univ. Press, Mar. 2015.

[14] S. Jivkova and M. Kavehrad, "Shadowing and blockage in indoor optical wireless communications," in *Proc. IEEE Global Telecommun. Conf. (GLOBECOM)*, San Francisco, CA, USA, vol. 6, Dec. 2003, pp. 3269–3273.

[15] L. Wu, Z. Zhang, J. Dang, and H. Liu, "Adaptive modulation schemes for visible light communications," *J. Lightw. Technol.*, vol. 33, no. 1, pp. 117–125, Jan. 1, 2015.

[16] V. Jungnickel, V. Pohl, S. Nonnig, and C. V. Helmolt, "A physical model of the wireless infrared communication channel," *IEEE J. Sel. Areas Commun.*, vol. 20, no. 3, pp. 631–640, Apr. 2002.

[17] A. M. Khalid, G. Cossu, R. Corsini, P. Choudhury, and E. Ciaramella, "1-Gb/s transmission over a phosphorescent white LED by using rate-adaptive discrete multitone modulation," *IEEE Photon. J.*, vol. 4, no. 5, pp. 1465–1473, Oct. 2012.

[18] E. Perahia and R. Stacey, *Next Generation Wireless LAN: 802.11n and 802.11ac*. Cambridge, U.K.: Cambridge Univ. Press, 2013.

[19] H. Burchardt, S. Sinanovic, Z. Bharucha, and H. Haas, "Distributed and autonomous resource and power allocation for wireless networks," *IEEE Trans. Commun.*, vol. 61, no. 7, pp. 2758–2771, Jul. 2013.

[20] D. Tsonev *et al.*, "A 3-Gb/s single-LED OFDM-based wireless VLC link using a gallium nitride μLED," *IEEE Photon. Technol. Lett.*, vol. 26, no. 7, pp. 637–640, Apr. 1, 2014.

[21] J. Mo and J. Walrand, "Fair end-to-end window-based congestion control," *IEEE/ACM Trans. Netw.*, vol. 8, no. 5, pp. 556–567, Oct. 2000.

[22] Q. Ye, B. Rong, Y. Chen, M. Al-Shalash, C. Caramanis, and J. G. Andrews, "User association for load balancing in heterogeneous cellular networks," *IEEE Trans. Wireless Commun.*, vol. 12, no. 6, pp. 2706–2716, Jun. 2013.

[23] A. Blenk, A. Basta, and W. Kellerer, "HyperFlex: An SDN virtualization architecture with flexible hypervisor function allocation," in *Proc. IFIP/IEEE Int. Symp. Integr. Netw. Manag. (IM)*, May 2015, pp. 397–405.

[24] S. Khan *et al.*, "Software-defined network forensics: Motivation, potential locations, requirements, and challenges," *IEEE Netw.*, vol. 30, no. 6, pp. 6–13, Nov./Dec. 2016.

[25] R. Vilalta *et al.*, "Multidomain network hypervisor for abstraction and control of OpenFlow-enabled multitenant multitechnology transport networks [Invited]," *IEEE/OSA J. Opt. Commun. Netw.*, vol. 7, no. 11, pp. B55–B61, Nov. 2015.

[26] E. Biglieri, G. Caire, and G. Taricco, *Coding for the Fading Channel: A Survey*. Amsterdam, The Netherlands: IOS Press, 1999.

[27] S. Sesia, I. Toufik, M. Baker eds., *LTE—The UMTS Long Term Evolution* (From Theory to Practice), Hoboken, NJ, USA: Wiley, 2009.

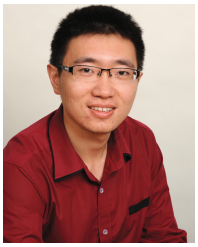

Yunlu Wang (S'14) received the B.Eng. degree in telecommunication engineering from the Beijing University of Post and Telecommunications, China, in 2011, and dual M.Sc. degrees in digital communication and signal processing from The University of Edinburgh, U.K., in 2013, and in electronic and electrical engineering from Beihang University, China, in 2014 respectively. He is currently pursuing the Ph.D. degree in electrical engineering with The University of Edinburgh. His research focus is on visible light communication and radio frequency hybrid networking.

Authorized licensed use limited to: CAMBRIDGE UNIV. Downloaded on November 18,2020 at 14:37:39 UTC from IEEE Xplore. Restrictions apply.

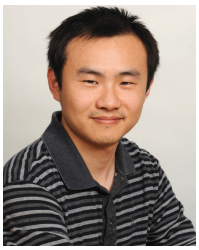

Xiping Wu (S'11–M'14) received the Ph.D. degree from The University of Edinburgh, Scotland, U.K., in 2015. From 2011 to 2014, he was a Marie-Curie Early-Stage Researcher funded by the European Union's Seventh Framework Program Project GREENET. Since 2014, he has been a Research Associate with the Institute for Digital Communications, The University of Edinburgh, funded by the British Engineering and Physical Sciences Research Council Project TOUCAN. His main research interests are in the areas of wireless communication theory, visible light communications, and wireless network management. In 2010, he received the Scotland Saltire Scholarship by the Scottish Government.

Harald Haas (S'98–AM'00–M'03) received the Ph.D. degree from The University of Edinburgh in 2001. He currently holds the Chair of Mobile Communications with The University of Edinburgh. He is a Co-Founder and the Chief Scientific Officer with pureLiFi Ltd. He holds 31 patents and has over 30 pending patent applications. He has authored 300 conference and journal papers, including a paper in *Science*. He first introduced and coined spatial modulation and Li-Fi. Li-Fi was listed among the 50 best inventions in the *TIME Magazine* in 2011. His main research interests are in optical wireless communications, hybrid optical wireless and RF communications, spatial modulation, and interference coordination in wireless networks. He was an invited speaker at TED Global in 2011, and his talk has been watched online over 1.5 million times. He was a recipient of the prestigious Established Career Fellowship from the Engineering and Physical Sciences Research Council (EPSRC) within Information and Communications Technology in the U.K., in 2012, and the Tam Dalyell Prize 2013 awarded by The University of Edinburgh for excellence in engaging the public with science. He was a co-recipient of the best paper award at the *IEEE Vehicular Technology Conference*, Las Vegas, in 2013, and Glasgow, in 2015. In 2014, he was selected by EPSRC as one of ten Recognizing Inspirational Scientists and Engineers Leaders.

Authorized licensed use limited to: CAMBRIDGE UNIV. Downloaded on November 18,2020 at 14:37:39 UTC from IEEE Xplore. Restrictions apply.